

NASA/CR-1998-208436  
ICASE Report No. 98-25

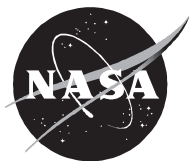


## **A New Time-space Accurate Scheme for Hyperbolic Problems I: Quasi-explicit Case**

*David Sidilkover*  
*ICASE, Hampton, Virginia*

*Institute for Computer Applications in Science and Engineering*  
*NASA Langley Research Center*  
*Hampton, VA*

*Operated by Universities Space Research Association*



National Aeronautics and  
Space Administration

Langley Research Center  
Hampton, Virginia 23681-2199

Prepared for Langley Research Center under  
Contracts NAS1-19480 and NAS1-97046

October 1998

# A NEW TIME-SPACE ACCURATE SCHEME FOR HYPERBOLIC PROBLEMS I: QUASI-EXPLICIT CASE\*

DAVID SIDILKOVER<sup>†</sup>

**Abstract.** This paper presents a new discretization scheme for hyperbolic systems of conservation laws. It satisfies the TVD property and relies on the new high-resolution mechanism which is compatible with the genuinely multidimensional approach proposed recently. This work can be regarded as a first step towards extending the genuinely multidimensional approach to unsteady problems. Discontinuity capturing capabilities and accuracy of the scheme are verified by a set of numerical tests.

**Key words.** unsteady problems, high-resolution schemes, TVD property.

**Subject classification.** Applied and Numerical Mathematics.

**1. Introduction.** A general approach towards the construction of genuinely multidimensional high-resolution schemes for hyperbolic systems was proposed recently ([16],[15],[17]). The main advantage of this approach is that it results in the discrete schemes that have some desirable properties which allow to design very efficient steady solvers (see [13] for a summary). However, these discretizations are suitable exclusively for steady problems since they are second order accurate at the steady-state only.

Extending of the genuinely multidimensional approach to the transient problems may seem at the first sight straightforward. Noting that the unsteady advection problem in one dimensions is very similar to the steady advection problem in two dimensions, one can apply, say, the “fluctuation-splitting” (or “residual distribution”) steady 2D advection scheme for triangular meshes (proposed in [3] and given an algebraic formulation using limiters in [19]) to a one dimensional unsteady problem as well. However, a closer look reveals that the result of such a straightforward application may be that the “present” depends on the “future”. One could leave the causality concerns to the philosophers and try to iterate back and forth in space-time. However, the memory requirements of this approach will become absurdly demanding in more than one spatial dimension, since all the time instances need to be stored.

This paper presents a new discrete scheme for the hyperbolic conservation laws and systems of conservation laws. It is one-step one-stage and satisfies the TVD property. The key feature of the new scheme is that it relies on the non-standard high-resolution mechanism which is compatible with the genuinely multidimensional approach proposed recently and will allow to extend it to unsteady problems. The scheme is formulated using the framework introduced by Sweby [21], which makes it plain what are the differences and similarities between the proposed and the existing discretizations. The new scheme has links to the 2D steady advection control volume scheme constructed in [14],[18]. As the first stage we address only the case of Courant number less than one. The constructed scheme is not explicit even in this case. However, the treatment of the discrete equations can be made sufficiently similar to explicit (see §3). That is why we call the approach “quasi-explicit”. We verify the accuracy and the discontinuity capturing properties of the new scheme and demonstrate that the quality of the solutions obtained using it is at least as good as when using the standard schemes.

---

\*This work was supported by the National Aeronautics and Space Administration under NASA Contract Nos. NAS1-19480 and NAS1-97046 while the author was in residence at the Institute for Computer Applications in Science and Engineering (ICASE), NASA Langley Research Center, Hampton, VA 23681-2199.

<sup>†</sup>ICASE, Mail Stop 403, NASA Langley Research Center, Hampton, VA 23681

The goal of this research direction is to construct very efficient implicit solvers for the unsteady compressible flow equations. The unsteady genuinely-multidimensional schemes are expected to allow this since they should maintain some fundamental properties of their steady ancestors: a good measure  $h$ -ellipticity of the implicit discretizations and the possibility to distinguish between different co-factors of the systems of equations. Therefore, the next step will be to consider the implicit case (Courant number larger than one) and to design an efficient implicit solver. This study will be reported elsewhere.

The paper is organized as follows: §2 contains the description of the scheme (in control volume formulation) and the discussion concerning some basic properties. A possible solution procedure for the discrete equations is presented in §3. Generalization of the scheme to the Euler system is given in §4. §5 reports the numerical tests conducted with the constructed scheme. Some conclusions and discussion regarding the future research directions are presented in §6. The residual-distribution (fluctuation-splitting) formulation of the scheme is given in Appendix A. Also a brief discussion on more general conditions for a scheme to be TVD is given in Appendix B.

**2. The new scheme and its basic properties.** Consider first an initial value problem for a scalar conservation law

$$(2.1) \quad \begin{aligned} u_t + f(u)_x &= 0, \quad t \geq 0, \quad x \in \mathbb{R}, \\ u(x, 0) &= u_0(x). \end{aligned}$$

Following Sweby [21] we shall use the following simplified notation (unless specified otherwise) for the data on the new and old time levels respectively

$$(2.2) \quad u^k \equiv u_k^{n+1}, \quad u_k \equiv u_k^n.$$

A general conservative discretization of (2.1) can be given as follows

$$(2.3) \quad u^k = u_k - \lambda(h_{k+\frac{1}{2}} - h_{k-\frac{1}{2}})$$

where  $h_{k+\frac{1}{2}}$  is the consistent numerical flux

$$(2.4) \quad \begin{aligned} h_{k+\frac{1}{2}} &= h(u_{k-m}, \dots, u_{k+m+1}, u^{k-m}, \dots, u^{k+m+1}) \\ h(u, \dots, u) &= f(u) \end{aligned}$$

and  $\lambda$  is the mesh ratio

$$(2.5) \quad \lambda = \frac{\Delta t}{\Delta x}.$$

A crucial property needed for convergence proof of the difference scheme (2.3) is the so-called *Total Variation Diminishing* (TVD) property [4]

$$(2.6) \quad TV(u^{n+1}) \leq TV(u^n),$$

where, abolishing temporarily the notation (2.2), we define the Total Variation an time level  $n$  as

$$(2.7) \quad TV(u^n) = \sum_n |u_{k+1}^n - u_k^n|$$

If the scheme (2.3) can be written in the form

$$(2.8) \quad u^k = u_k - C_{k-\frac{1}{2}} \Delta u_{k-\frac{1}{2}} + D_{k+\frac{1}{2}} \Delta u_{k+\frac{1}{2}},$$

then a sufficient condition for the scheme to be TVD (Harten's Lemma, see [4]) is that the (data-dependent) coefficients satisfy the inequalities

$$(2.9) \quad 0 \leq C_{k+\frac{1}{2}}, \quad 0 \leq D_{k+\frac{1}{2}},$$

and

$$(2.10) \quad 0 \leq C_{k+\frac{1}{2}} + D_{k+\frac{1}{2}} \leq 1.$$

**2.1. First order upwind scheme.** Consider first for the purpose of illustration the first order upwind scheme.

Define the local propagation speed

$$(2.11) \quad a_{k+\frac{1}{2}} = \frac{\Delta f_{k+\frac{1}{2}}}{\Delta u_{k+\frac{1}{2}}}$$

where

$$(2.12) \quad \Delta f_{k+\frac{1}{2}} = f(u_{k+1}) - f(u_k), \quad \Delta u_{k+\frac{1}{2}} = u_{k+1} - u_k.$$

A numerical flux defining a first order upwind scheme can be written as follows

$$(2.13) \quad h_{k+\frac{1}{2}}^u = \frac{1}{2}[(f(u_k) + f(u_{k+1})) - |a_{k+\frac{1}{2}}|\Delta u_{k+\frac{1}{2}}].$$

Denote

$$(2.14) \quad \begin{aligned} a_{k+\frac{1}{2}}^+ &= \frac{1}{2}(a_{k+\frac{1}{2}} + |a_{k+\frac{1}{2}}|) \\ a_{k+\frac{1}{2}}^- &= \frac{1}{2}(a_{k+\frac{1}{2}} - |a_{k+\frac{1}{2}}|) \end{aligned}$$

and

$$(2.15) \quad \begin{aligned} \nu_{k+\frac{1}{2}}^+ &= \lambda a_{k+\frac{1}{2}}^+ \\ \nu_{k+\frac{1}{2}}^- &= \lambda a_{k+\frac{1}{2}}^- \end{aligned}$$

The local CFL number then can be written as follows

$$(2.16) \quad \nu_{k+\frac{1}{2}} = \lambda a_{k+\frac{1}{2}} = \nu_{k+\frac{1}{2}}^+ + \nu_{k+\frac{1}{2}}^-.$$

It is easy to see that using (2.14),(2.15) the scheme defined by (2.13) will read as

$$(2.17) \quad u^k = u_k - \nu_{k-\frac{1}{2}}^+ \Delta u_{k-\frac{1}{2}} - \nu_{k+\frac{1}{2}}^- \Delta u_{k+\frac{1}{2}}$$

Denoting

$$(2.18) \quad C_{k+\frac{1}{2}} = \nu_{k+\frac{1}{2}}^+, \quad D_{k+\frac{1}{2}} = -\nu_{k+\frac{1}{2}}^-$$

makes it obvious that inequality (2.9) is satisfied, and that

$$(2.19) \quad C_{k+\frac{1}{2}} + D_{k+\frac{1}{2}} = \nu_{k+\frac{1}{2}}^+ - \nu_{k+\frac{1}{2}}^- = |\nu_{k+\frac{1}{2}}| \leq 1$$

is a CFL condition. Therefore, the first order upwind scheme is TVD.

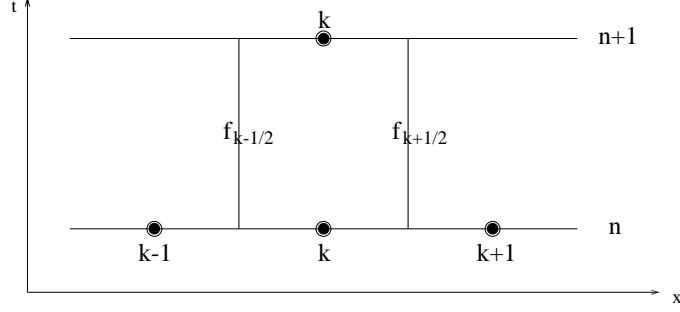


FIG. 1. Stencil of the Lax-Wendroff scheme.

**2.2. The high-resolution scheme: constant coefficient equation.** In order to illustrate the construction of a high-resolution scheme we shall consider first a linear constant coefficient equation

$$(2.20) \quad u_t + au_x = 0, \quad a > 0.$$

The first order upwind scheme approximating (2.20) can be written as follows

$$(2.21) \quad u^k = u_k - \nu \Delta u_{k-\frac{1}{2}}$$

where

$$(2.22) \quad \nu = \frac{a\Delta t}{\Delta x}$$

is the CFL number. The second order Lax-Wendroff [6] scheme can be given as follows (the corresponding stencil is depicted on Fig.1)

$$(2.23) \quad u^k = u_k - \nu \Delta u_{k-\frac{1}{2}} - \Delta_- \left[ \frac{1}{2} (1 - \nu) \nu \Delta u_{k+\frac{1}{2}} \right]$$

or as a first order upwind scheme (2.21) whose flux (2.13) is augmented by the following anti-diffusive flux

$$(2.24) \quad -\frac{1}{2\lambda} (1 - \nu) \nu \Delta u_{k+\frac{1}{2}}$$

**2.2.1. Some existing schemes.** The Lax-Wendroff (as well as any second order linear scheme) is known not to satisfy the TVD property. A high-resolution scheme can be defined by adding a “limited” anti-diffusive flux to the first order upwind one. The resulting scheme reads as follows

$$(2.25) \quad u^k = u_k - \nu \Delta u_{k-\frac{1}{2}} - \Delta_- \left[ \psi(q_k) \frac{1}{2} (1 - \nu) \nu \Delta u_{k+\frac{1}{2}} \right],$$

where  $q_k$  is standardly defined as a ratio of two subsequent finite differences of the numerical solution on the time-level  $n$

$$(2.26) \quad q_k = \frac{\Delta u_{k-\frac{1}{2}}}{\Delta u_{k+\frac{1}{2}}}.$$

Noting that the following identity holds

$$(2.27) \quad \psi(q_k) \Delta u_{k+\frac{1}{2}} \equiv \frac{\psi(q_k)}{q_k} \Delta u_{k-\frac{1}{2}},$$

it can be concluded (see [21]) that high-resolution scheme (2.25) can be viewed as a nonlinear hybrid of Lax-Wendroff and the Warming-Beam [22] schemes. The latter is given by the following (the stencil is depicted

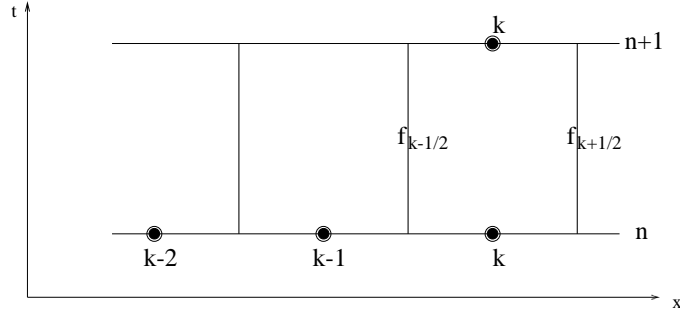


FIG. 2. Stencil of the Warming-Beam scheme.

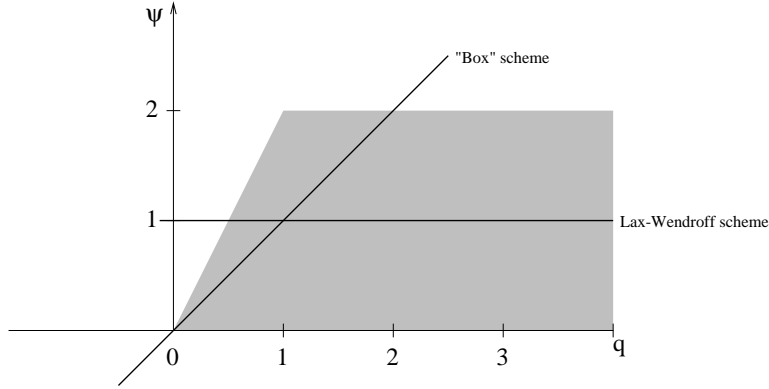


FIG. 3. TVD region.

at Fig.2)

$$(2.28) \quad u^k = u_k - \nu \Delta u_{k-\frac{1}{2}} - \Delta_- \left[ \frac{1}{2} (1 - \nu) \nu \Delta u_{k-\frac{1}{2}} \right]$$

It was also shown in [21] that the high-resolution scheme (2.25) is TVD provided the limiter function  $\psi$  satisfies the following requirements

$$(2.29) \quad 0 \leq \psi(q) \leq 2, \quad 0 \leq \frac{\psi(q)}{q} \leq 2$$

The common practice is also to require

$$(2.30) \quad \psi(q) = 0, \quad q \leq 0.$$

Hence (see [21]) if the limiter function lies within the “shaded” area shown on Fig.3, scheme (2.25) satisfies TVD property. Requiring the scheme also to be second order accurate wherever possible implies that  $\psi(q)$  has to be a Lipschitz-continuous function and

$$(2.31) \quad \psi(1) = 1.$$

It is also desirable (see [21]) that the resulting non-linear high-resolution scheme is an *internal* average of the Lax-Wendroff and Warming-Beam scheme. Therefore, we obtain the second order subset of the TVD region as depicted on Fig.4.

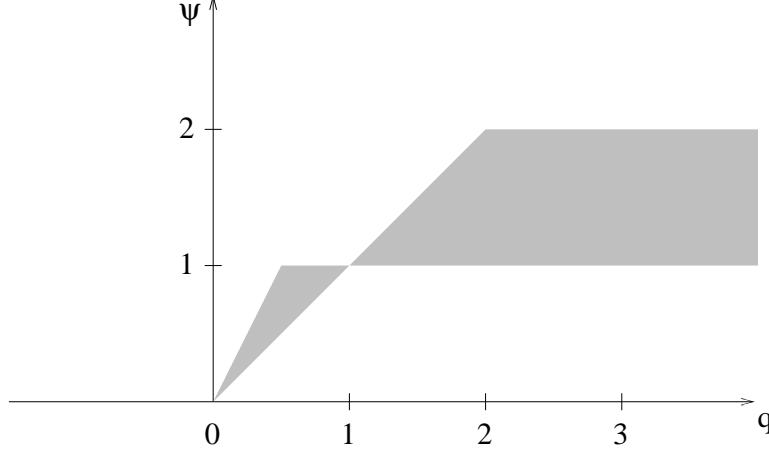


FIG. 4. Second order TVD region.

**2.2.2. The new high-resolution scheme.** Define the argument of the limiter function in the following way

$$(2.32) \quad q_k = -\frac{\Delta_t u_k}{\nu \Delta u_{k+\frac{1}{2}}}$$

where

$$(2.33) \quad \Delta_t u_k = u^k - u_k$$

is a finite difference of the numerical solution values at times  $n+1$  and  $n$  at point  $k$ . In other words, the limiter function in the new scheme relies on the ratio of the finite differences in *time* and *space* (each taken with an appropriate coefficient).

The identity

$$(2.34) \quad \psi(q_k) \nu \Delta u_{k+\frac{1}{2}} \equiv -\frac{\psi(q_k)}{q_k} \Delta_t u_k$$

allows to rewrite scheme (2.25),(2.32) in the following form

$$(2.35) \quad u^k = u_k - \nu \Delta u_{k-\frac{1}{2}} - \frac{1}{2}(1-\nu) \left[ -\frac{\psi(q_k)}{q_k} \Delta_t u_k + \frac{\psi(q_{k-1})}{q_{k-1}} \Delta_t u_{k-1} \right],$$

suggesting that the scheme (2.25),(2.32) (whose stencil is represented by Fig.6) can be viewed as a nonlinear hybrid of the Lax-Wendroff and the “box” schemes. The latter is given by the following

$$(2.36) \quad u^k = u_k - \nu \Delta u_{k-\frac{1}{2}} - \frac{1}{2}(1-\nu) [-\Delta_t u_k + \Delta_t u_{k-1}]$$

and its stencil is depicted on Fig.5.

Using (2.34), we can rewrite (2.25),(2.32) as follows

$$(2.37) \quad u^k = u_k - \nu \Delta u_{k-\frac{1}{2}} - \frac{1}{2}(1-\nu) \left[ -\frac{\psi(q_k)}{q_k} \Delta_t u_k - \psi(q_{k-1}) \nu \Delta u_{k-\frac{1}{2}} \right],$$

or

$$(2.38) \quad u^k = u_k - \nu \frac{1 - \frac{1}{2}(1-\nu)\psi(q_{k-1})}{1 - \frac{1}{2}(1-\nu)\psi(q_k)/q_k} \Delta u_{k-\frac{1}{2}}.$$

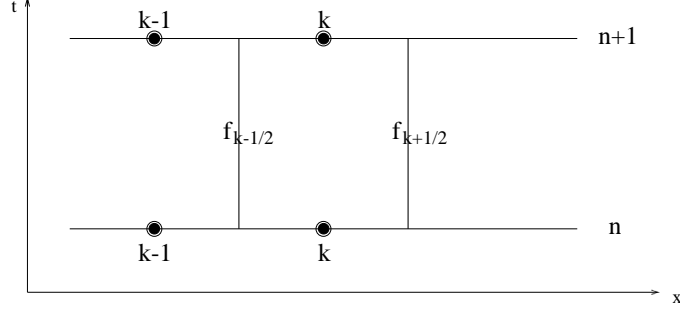


FIG. 5. Stencil of the “Box” scheme.

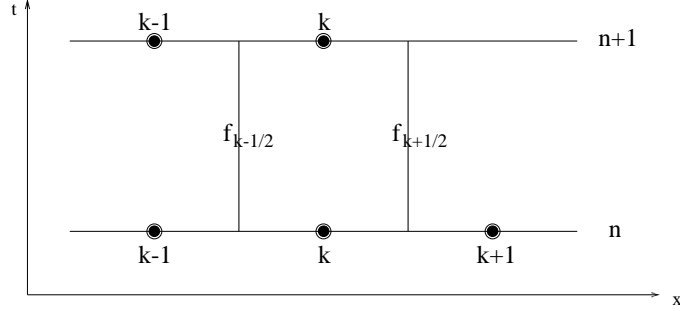


FIG. 6. Stencil of the new high-resolution scheme.

The latter can be written in the form (2.8) with

$$(2.39) \quad C_{k-\frac{1}{2}} = \nu \frac{1 - \frac{1}{2}(1 - \nu)\psi(q_{k-1})}{1 - \frac{1}{2}(1 - \nu)\psi(q_k)/q_k},$$

and

$$(2.40) \quad D_{k+\frac{1}{2}} = 0$$

It can be easily verified that the inequality (assuming  $\nu \leq 1$ )

$$(2.41) \quad 0 \leq C_{k-\frac{1}{2}} \leq 1$$

is equivalent to the following

$$(2.42) \quad \psi(q) \leq \frac{2}{1 - \nu}, \quad \text{and} \quad \frac{\psi(q)}{q} - \nu\psi(q) \leq 2,$$

which, in its turn, is satisfied if (2.29) holds.

**REMARK 2.1.** *The idea of using the “box” scheme as one of the building blocks when constructing a discretization for hyperbolic problem can be found in [9]. It is employed for the case of  $CFL > 1$ , while the Lax-Wendroff scheme is used when  $CFL \leq 1$ .*

**2.3. General case.** The new high-resolution scheme for general nonlinear problem (2.1) can be defined by adding a limited anti-diffusive flux to that of the first order upwind scheme (2.17) (as it was done previously for the linear constant coefficient case)

$$(2.43) \quad h_{k+\frac{1}{2}} = h_{k+\frac{1}{2}}^u + \frac{1}{2}(1 - \nu_{k+\frac{1}{2}}) \left( \psi(q_k^+) a_{k+\frac{1}{2}}^+ + \psi(q_{k+1}^-) a_{k+\frac{1}{2}}^- \right) \Delta u_{k+\frac{1}{2}},$$

where

$$(2.44) \quad q_k^+ = -\frac{\Delta_t u_k}{\lambda a_{k+\frac{1}{2}}^+ \Delta u_{k+\frac{1}{2}}}$$

and

$$(2.45) \quad q_{k+1}^- = -\frac{\Delta_t u_{k+1}}{\lambda a_{k+\frac{1}{2}}^- \Delta u_{k+\frac{1}{2}}}.$$

Using the identities

$$(2.46) \quad \psi(q_k^+) a_{k+\frac{1}{2}}^+ \Delta u_{k+\frac{1}{2}} \equiv -\frac{\psi(q_k^+)}{q_k^+} \frac{\Delta_t u_k}{\lambda}$$

and

$$(2.47) \quad \psi(q_{k+1}^-) a_{k+\frac{1}{2}}^- \Delta u_{k+\frac{1}{2}} \equiv -\frac{\psi(q_{k+1}^-)}{q_{k+1}^-} \frac{\Delta_t u_{k+1}}{\lambda},$$

the alternative form of the numerical flux (2.43) can be obtained

$$(2.48) \quad h_{k+\frac{1}{2}} = h_{k+\frac{1}{2}}^u - \frac{1}{2}(1 - \nu_{k+\frac{1}{2}}^+) \left( \frac{\psi(q_k^+)}{q_k^+} \frac{\Delta_t u_k}{\lambda} + \frac{\psi(q_{k+1}^-)}{q_{k+1}^-} \frac{\Delta_t u_{k+1}}{\lambda} \right).$$

Define

$$(2.49) \quad \mu_{k+\frac{1}{2}}^+ = \frac{1}{2} \psi(q_k) \nu_{k+\frac{1}{2}}^+ (1 - \nu_{k+\frac{1}{2}}^+), \quad \bar{\mu}_{k+\frac{1}{2}}^+ = \frac{1}{2} \frac{\psi(q_k)}{q_k} (1 - \nu_{k+\frac{1}{2}}^+)$$

and

$$(2.50) \quad \mu_{k+\frac{1}{2}}^- = \frac{1}{2} \psi(q_{k+1}) \nu_{k+\frac{1}{2}}^- (1 - \nu_{k+\frac{1}{2}}^-), \quad \bar{\mu}_{k+\frac{1}{2}}^- = \frac{1}{2} \frac{\psi(q_{k+1})}{q_{k+1}} (1 - \nu_{k+\frac{1}{2}}^-).$$

Denoting

$$(2.51) \quad C_{k-\frac{1}{2}} = \frac{\nu_{k-\frac{1}{2}}^+ (1 - \mu_{k-\frac{1}{2}}^+)}{1 - \bar{\mu}_{k-\frac{1}{2}}^+ - \bar{\mu}_{k+\frac{1}{2}}^-}$$

and

$$(2.52) \quad D_{k+\frac{1}{2}} = \frac{\nu_{k+\frac{1}{2}}^- (1 - \mu_{k+\frac{1}{2}}^-)}{1 - \bar{\mu}_{k-\frac{1}{2}}^+ - \bar{\mu}_{k+\frac{1}{2}}^-},$$

the scheme (2.3) with numerical fluxes defined by (2.43) (or (2.48)) can be put into form (2.8).

Finally, we can state the following result

**THEOREM 2.2.** *Scheme (2.3) with high resolution flux (2.43) that incorporates a limiter function satisfying (2.29) is TVD.*

*Proof.* Note that if  $\nu_{k-\frac{1}{2}}^+ > 0$ , then  $\bar{\mu}_{k-\frac{1}{2}}^+ = 0$ . Also, if  $\nu_{k+\frac{1}{2}}^+ > 0$ , then  $\bar{\mu}_{k+\frac{1}{2}}^+ = 0$ . It follows from here that

$$(2.53) \quad C_{k-\frac{1}{2}} \geq 0, \quad D_{k+\frac{1}{2}} \geq 0,$$

provided the limiter function  $\psi$  satisfies inequality (2.29).

Inequality (2.29) gives the following

$$(2.54) \quad C_{k+\frac{1}{2}} \leq 1, \quad D_{k+\frac{1}{2}} \leq 1,$$

However, since either  $\nu_{k+\frac{1}{2}}^+$  or  $\nu_{k+\frac{1}{2}}^-$  vanishes, either  $C_{k+\frac{1}{2}}$  or  $D_{k+\frac{1}{2}}$  will vanish as well. Therefore,

$$(2.55) \quad C_{k+\frac{1}{2}} + D_{k+\frac{1}{2}} \leq 1,$$

which together with (2.53) completes the proof.  $\square$

**REMARK 2.3.** Notice that a purely upwind decomposition (2.44)-(2.45) is necessary here for the construction, as the ratio between the numerator and denominator must be close to 1 in smooth monotone regions in order to keep accuracy. In particular, a Lax-Friedrichs type splitting cannot be used here.

**3. Solution procedure.** Consider for simplicity scheme (2.25) with (2.32), devised for linear problem (2.20). This scheme is not explicit – the stencil involves more than one point on the new time level  $n+1$  (Fig.6). However, there is no need for a global solver in this case. One can use some simple local procedures for solving procedures for solving the resulting discrete equations.

*Space marching.*

An obvious possibility is a space marching, i.e. solve the discrete equation at point  $k$  after it has been solved at point  $k-1$ . However, considering solving the nonlinear systems of equations and/or extensions to multi-dimensions, it appears that the latter method may be not always feasible/desirable.

*Predictor-Corrector.*

Consider an initial-boundary value problem for (2.20) discretized on a grid  $k = 0, \dots, K$ . Assume, that  $u_k$ , the solution on the time level  $n$ , is a monotonic function.

Consider an arbitrary discrete function  $u^{k\dagger}$  as an initial guess for a solution at the time level  $n+1$ . Performing one sweep of Jacobi relaxation using scheme (2.25) with (2.32) will result in  $u^{k*}$ ,  $i = 0, \dots, K$ . We can state the following

**LEMMA 3.1.** *If the discrete function  $u_k$ ,  $k = 0, \dots, K$  is monotonic, then the discrete function  $u^{k*}$  is monotonic as well.*

*Proof.* Putting scheme (2.25), (2.32) into form (2.8) with  $C_{k-\frac{1}{2}}$ ,  $D_{k+\frac{1}{2}}$  defined by (2.39), (2.41) and (2.39) respectively, we can conclude that

$$(3.1) \quad \min(u_{k-1}, u_k) \leq u^{k*} \leq \max(u_{k-1}, u_k),$$

which concludes the proof.  $\square$

This suggests that the following *predictor-corrector* procedure can be used for solving the discrete equations resulting from the limited scheme:

**Predictor.** Lax-Wendroff scheme to produce a grid-function  $u^{k\dagger}$ ,  $k = 0, \dots, K$ , which is a second order accurate solution to (2.1), but may exhibit an oscillatory behavior near discontinuities;

**Corrector.** Perform a Jacobi relaxation to update values  $u^{k\dagger}$  to obtain a new grid-function  $u^k$ ,  $k = 0, \dots, K$  that is non-oscillatory (due to Lemma 3.1) and second order accurate solution to (2.1).

Such a solution procedure is essentially a point-implicit solver. Note that the resulting discrete function may not in general satisfy the discrete equations corresponding either to the limited scheme or to the Lax-Wendroff scheme.

This should not cause any problems in the smooth regions since the discrepancy between the solutions to two different second order schemes is expected to second order small.

The difficulty though may arise in the vicinity of discontinuities. Different schemes may result in different discontinuity profiles. Therefore, if the residuals of one scheme are measured on the solution corresponding to another scheme, they may be large. If no special care is taken, this may have a cumulative effect over several time-steps and lead to wrong shock speeds.

Our experience though demonstrates, that it is sufficient to perform a few (instead of one) updates of the solution in the vicinity of a discontinuity using the “limited” scheme to make sure that the residuals of this scheme are very small. We shall elaborate on this issue in the future publication which will address also the implicit case.

**4. Hyperbolic systems.** We shall briefly sketch out an extension of the new scheme to the hyperbolic systems of conservation laws, in particular, to the Euler equations of gas dynamics

$$(4.1) \quad \mathbf{u}_t + \mathbf{f}(\mathbf{u})_x = 0$$

Again, as in the scalar case, the discretization can be put into the following general form

$$(4.2) \quad \mathbf{u}^k = \mathbf{u}_k - \lambda(\mathbf{h}_{k+\frac{1}{2}} - \mathbf{h}_{k-\frac{1}{2}})$$

$$(4.3) \quad \mathbf{u}^k \equiv \mathbf{u}_k^{n+1}, \quad \mathbf{u}_k \equiv \mathbf{u}_k^n$$

For the case of the Euler equations we can take the Roe-averaged Jacobian matrix of  $\mathbf{f}$  (see [11])

$$(4.4) \quad \tilde{A}_{k+\frac{1}{2}}(\mathbf{u}_{k+1} - \mathbf{u}_k) = \mathbf{f}(\mathbf{u}_{k+1}) - \mathbf{f}(\mathbf{u}_k)$$

and define the first order upwind flux as follows

$$(4.5) \quad \mathbf{h}_{k+\frac{1}{2}}^u = \frac{1}{2}[(\mathbf{f}(\mathbf{u}_k) + \mathbf{f}(\mathbf{u}_{k+1})) - |\tilde{A}_{k+\frac{1}{2}}|(\mathbf{u}_{k+1} - \mathbf{u}_k)]$$

Here

$$(4.6) \quad |\tilde{A}_{k+\frac{1}{2}}| = T|\Lambda|T^{-1},$$

$T$  is the matrix of right eigenvectors of  $A$ , and

$$(4.7) \quad \Lambda = T^{-1}\tilde{A}_{k+\frac{1}{2}}T,$$

is a diagonal matrix

$$(4.8) \quad \Lambda = \text{diag}\{a_1, \dots, a_n\}$$

and its absolute value is defined as

$$(4.9) \quad |\Lambda| = \text{diag}\{|a_1|, \dots, |a_n|\}.$$

We define the flux corresponding to the new high-resolution scheme as

$$(4.10) \quad \mathbf{h}_{k+\frac{1}{2}} = \mathbf{h}_{k+\frac{1}{2}}^u + \frac{1}{2}T^{-1}\mathbf{h}_{k+\frac{1}{2}}^{AD}$$

where the anti-diffusive flux is given by

$$(4.11) \quad \mathbf{h}^{AD} = (h_1, \dots, h_n)^T$$

and

$$(4.12) \quad (h_i)_{k+\frac{1}{2}} = (1 - (\nu_i)_{k+\frac{1}{2}}) \left( \psi((q_i)_k^+) (a_i)_{k+\frac{1}{2}}^+ + \psi((q_i)_{k+1}^-) (a_i)_{k+\frac{1}{2}}^- \right) \Delta(w_i)_{k+\frac{1}{2}}$$

with

$$(4.13) \quad (\nu_i)_{k+\frac{1}{2}} = \frac{a_i \Delta t}{\Delta x},$$

$$(4.14) \quad (q_i)_k^+ = -\frac{\Delta_t(w_i)_k}{\lambda(a_i)_{k+\frac{1}{2}}^+ \Delta(w_i)_{k+\frac{1}{2}}},$$

$$(4.15) \quad (q_i)_{k+1}^- = -\frac{\Delta_t(w_i)_{k+1}}{\lambda(a_i)_{k+\frac{1}{2}}^- \Delta(w_i)_{k+\frac{1}{2}}}$$

and  $(\nu_i)_{k+\frac{1}{2}}^+$  and  $(\nu_i)_{k+\frac{1}{2}}^-$  are the “positive” and “negative” parts of  $(\nu_i)_{k+\frac{1}{2}}$  respectively.

REMARK 4.1. *Note that the formulated scheme (as well as any other scheme based on the pure upwind decomposition) may produce non-physical solutions violating the entropy condition. Some ways to fix this problem have been described in the literature (see, for instance, [5]). Therefore, we do not include a discussion on this matter here.*

**5. Numerical results.** In this section we present some numerical tests of the new scheme using a few standard test problems.

### 5.1. Scalar case.

**5.1.1. Linear advection equation.** The purpose of this test is to verify the second order accuracy of the method. Therefore, we use here a simple problem with the known exact solution.

Consider the initial-boundary value problem for the following equation

$$(5.1) \quad u_t + .5u_x = 0.$$

on the domain  $[-1, 1]$  with the initial condition given by

$$(5.2) \quad u(x, 0) = -.5 \sin \pi x + .5$$

and the boundary condition (at point  $x = -1$ )

$$(5.3) \quad u(-1, t) = .5 \sin(1 + .5t) + .5.$$

It is obvious that the exact solution to this problem is given by

$$(5.4) \quad u = -.5 \sin \pi(x - .5t) + .5.$$

The  $L_1$  error norm of the solution error at time  $t = 1.0$  for different levels of resolution is presented in Table 5.1. The Courant number in all the tests is .5. The error reduction due to the doubling of the number of the grid-points is roughly by factor 4, which verifies that the scheme is second order accurate for smooth solutions.

TABLE 5.1  
*Linear advection equation: solution error  $L_1$  norm behavior with the mesh refinement.*

Number of grid-points	Solution error ( $L_1$ norm)	Numerical order of accuracy
25	0.0075311723	
50	0.0018290140	2.042
100	0.0004250877	2.106
200	0.0000971690	2.129

TABLE 5.2  
*Burgers equation: solution error  $L_1$  norm behavior with the mesh refinement.*

Number of grid-points	Solution error ( $L_1$ norm)	Numerical order of accuracy
50	0.0020134142	
100	0.0005068036	1.990
200	0.0001261164	2.007

**5.1.2. Burgers equation.** Our next purpose is to examine the accuracy of the new scheme as well as its capability to resolve shocks, representing them by a sharp oscillation-free profile. The problem considered here is the following nonlinear conservation law

$$(5.5) \quad u_t + .5(u^2)_x = 0.$$

The following expression (raised sine) serves as the initial condition

$$(5.6) \quad u(x, 0) = -\sin(\pi x) + 0.5$$

First we demonstrate the accuracy of the scheme for time  $t = .25$  by comparing the solution error norm for different levels of resolution (see Table 5.2). In this case the solution is still smooth, since the shock did not start to develop yet. The ability of the scheme to resolve shocks is demonstrated on the same test problem. The numerical solution to this problem corresponding to time  $t = 2$  is presented on Fig. 7. We can see that the shock is represented by a sharp layer and that there are no over- and undershoots on its sides.

**5.2. Euler equations.** In this section we present some numerical tests of the new scheme using a few standard test problems concerning the Euler equations of gas dynamics. The scheme used is as described in §4 with the Van Albada limiter. Note, that the Van Albada limiter does not satisfy the inequalities (2.29) (see Fig. 12), which are a sufficient condition for a (scalar) scheme to be TVD. A more general sufficient condition, that is satisfied by the Van Albada limiter, is presented in Appendix B. The reasons for using the Van Albada limiter is discussed in Appendix B as well.

All the test-cases considered here use the domain  $\mathcal{D} = \{x : x \in [-1, 1]\}$ .

*Lax's problem.* The initial data for this problem are two constant states, one to the left of the origin ( $-1 \leq x \leq 0$ ):  $\rho_l = .445, q_l = .698, P_l = 3.528$ , another to the right of the origin ( $0 \leq x \leq 1$ ):  $\rho_r = .5, q_r = 0, P_r = .571$ . Here  $\rho$  stands for density,  $q$  for velocity and  $P$  for pressure.

The numerical results for this case are presented on Fig. 8. The computational grid is 200 points. Solid lines represent the exact solution to the problem.

*Sod's problem.* Similarly to the previous problem, the initial data are given for the two constant states:  $\rho_l = 1, q_l = 0, P_l = 1$  and  $\rho_r = .125, q_r = 0, P_r = .1$ .

The grid consists of 200 points and the solid line represents the exact solution.

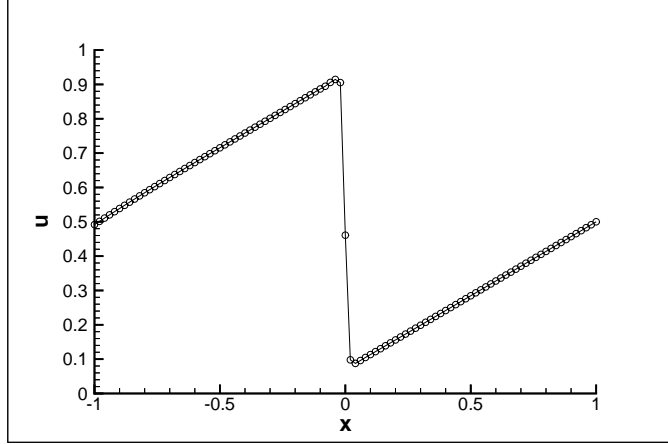


FIG. 7. Burgers equation. A numerical solution obtained on a grid of 100pts. at time  $t = 2$ . The initial condition is given by (5.6).

*Shock interacting with a disturbance in density (the testcase by Shu & Osher [12]).* The initial data for this problem is  $\rho_l = 3.857143, q_l = 2.629367, P_l = 10.33333$  for  $-1 \leq x \leq -.8$  and  $\rho_r = 1 + .2 \sin(5\pi x), q_r = 0, P_r = 1$  for  $-.8 \leq x \leq 1$ .

The interaction of the moving shock with a sinusoidal disturbance in density generates higher frequencies in the post-shock area. Here we test a capability of the new scheme to resolve these oscillations. The numerical experiments use three different levels of resolution (see Fig.10a,b,c). The solid line represents a numerical solution obtained on a very fine grid (1600 points). The snapshots correspond to time  $t = .36$ .

*Colella-Woodward problem.* The initial data for this problem is given by three constant states:  $\rho_l = 1, q_l = 0, P_l = 1000$  for  $-1 \leq x \leq -.8$ ,  $\rho_m = 1, q_m = 0, P_m = .01$  for  $-.8 \leq x \leq .8$  and  $\rho_r = 1, q_r = 0, P_r = 100$  for  $.8 \leq x \leq 1$ . Results are shown on Fig.11 (time  $t = .75$ ).

**6. Conclusions.** A new discretization scheme for hyperbolic problems was presented. It can be viewed as high-resolution generalization of the Lax-Wendroff scheme. In this paper we consider only the case of Courant number less than unity. Even in this case the resulting scheme is implicit. However, we demonstrate that the solution procedure in this case does not have to involve a implicit global solver, but can rely on some simple local techniques. That is why we call this case *quasi-explicit*.

The methodology incorporated into the new high-resolution mechanism should allow to extend the previously proposed genuinely multidimensional approach (see [16, 15, 17]) to unsteady problems. This is a subject of the future study.

Another very promising direction is to generalize the scheme for the case of Courant number larger than unity. The procedure of solving the discrete equations in this case may require a global implicit solver.

The properties of the genuinely multidimensional (steady) schemes summarized in [13], however, indicate that extremely efficient implicit solvers can be constructed for unsteady generalizations of such schemes as well. This is another major direction for the future research.

It is also interesting to note that the schemes proposed by Colella [1, 2], LeVeque [7],[8] and Radvogin [10] can all be regarded as extensions to multi-dimensions of scheme (2.25) with the standard limiters with the argument given by (2.26). The genuinely multidimensional scheme (in the spirit of [15] when extended to unsteady problems can be viewed as extension of the scheme presented in this paper, namely, (2.25) with the limiters relying on the ratio of differences in space and time (2.32).

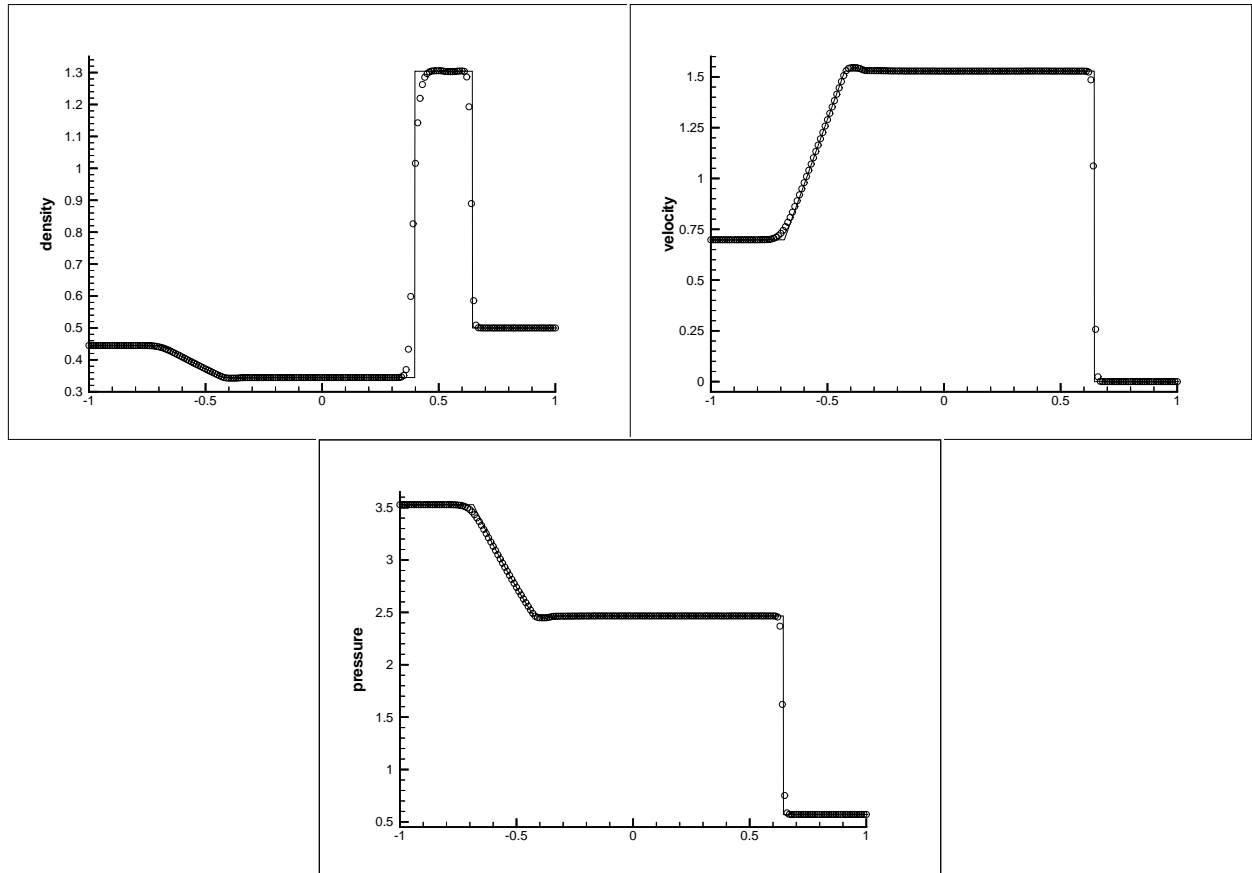


FIG. 8. *Lax's problem. A numerical solution obtained on a grid of 200pts. is represented by circles. The solid line corresponds to the exact solution.*

Consider a transient problem that converges to a steady-state. It is interesting to note that if the Lax-Wendroff scheme (or one of its standard generalizations) is applied to solve such a problem, the computed steady-state solution will depend on the time-step (since the artificial dissipation of such schemes scales with the time-step). The scheme proposed in this paper, however (even though it is an extension of the Lax-Wendroff scheme), will produce a steady-state solution that is independent of the time-step. This is due to the fact that if the temporal changes of the solution become very small and eventually vanish, the limiter will cut off all the spatial terms in the discretization that scale with the time-step. Thus, the scheme essentially reduces to the first order upwind. The generalization of the scheme presented here to multi-dimensions is expected to maintain this property to a certain extent as well.

**Acknowledgments.** The author would like to thank Chi-Wang Shu and Randall LeVeque for reading the manuscript and making numerous very helpful comments.

## REFERENCES

- [1] P. COLELLA, *Multidimensional upwind methods for hyperbolic conservation laws*, Tech. Rep. LBL-17023, Lawrence Berkeley Report, 1984.
- [2] ———, *Multidimensional upwind methods for hyperbolic conservation laws*, J. Comp. Phys., 87 (1990), p. 171.

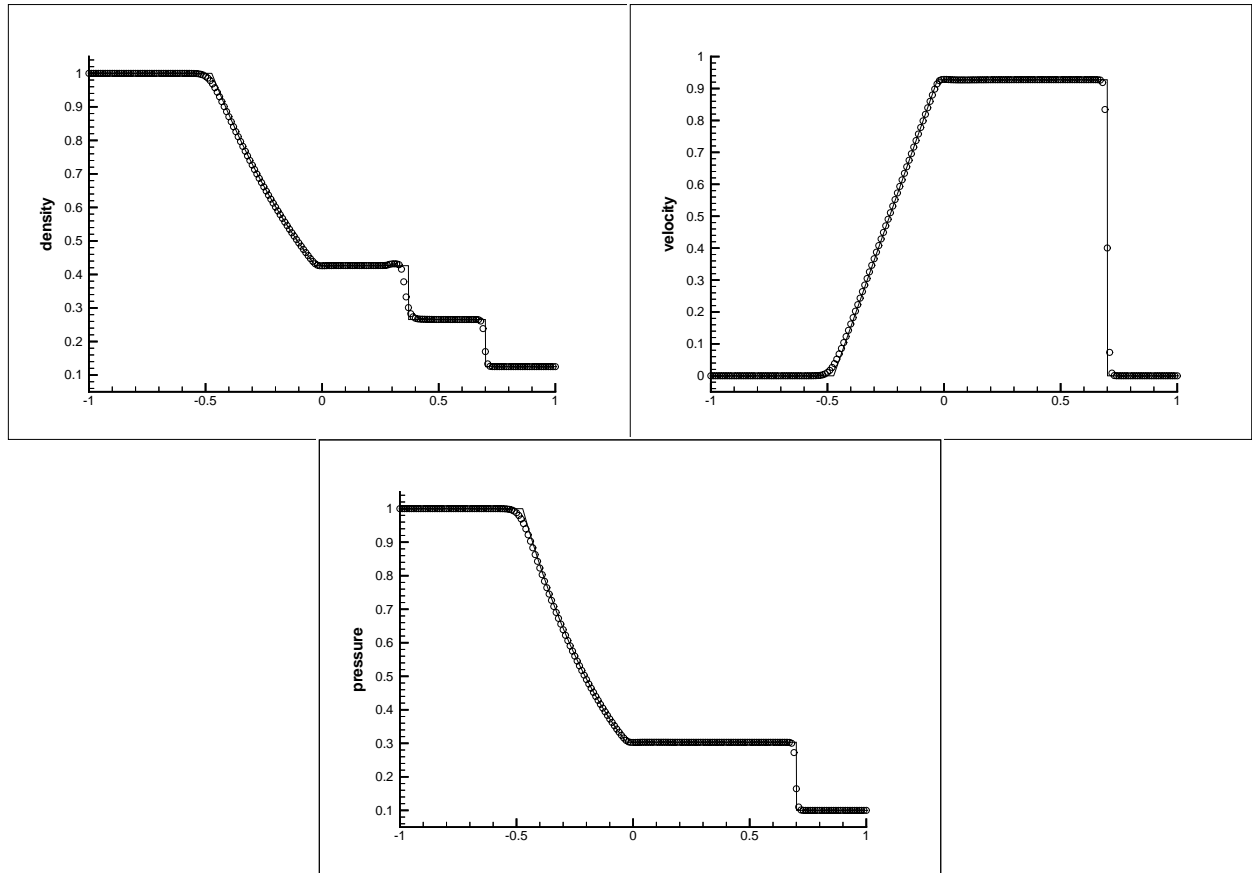


FIG. 9. Sod's problem. A numerical solution on 200pts. grid is depicted by circles. The exact solution is represented by the solid line.

- [3] H. DECONINCK, R. STRUIJS, AND P. L. ROE, *Fluctuation splitting for multidimensional convection problem: an alternative to finite volume and finite element methods*, vki lecture series 1990-3 on computational fluid dynamics, Von Karman Institute, Brussels, Belgium, March 1991.
- [4] A. HARTEN, *High resolution schemes for hyperbolic conservation laws*, J. Comp. Phys., 49 (1983), pp. 357–393.
- [5] A. HARTEN AND J. HYMAN, *Self-adjusting grid for one-dimensional hyperbolic conservation laws*, J. Comp. Phys., 50 (1983), pp. 235–269.
- [6] P. D. LAX AND B. WENDROFF, *Systems of conservation laws*, Comm. Pure Appl. Math., 13 (1960), pp. 217–237.
- [7] R. J. LEVEQUE, *High resolution finite volume methods on arbitrary grids via wave propagation*, J. Comp. Phys., 78 (1988).
- [8] R. J. LEVEQUE, *Wave propagation algorithms for multi-dimensional hyperbolic systems*, J. Comput. Phys., 131 (1997), pp. 327–353.
- [9] Y. B. RADVOGIN, *Reshenie smeshannoi zadachi dlya giperbolicheskikh sistem i uravnenii gazovoi dinamiki s pomoschyu yavno-neyavnoi shemi vtorogo poryadka (in Russian)*, Preprint No. 8, Keldysh Institute of Applied Mathematics, Soviet Academy of Science, 1987.
- [10] —, *Quasi-monotonous multidimensional difference schemes with second order accuracy*. Soviet Academy of Science Preprint, 1991.

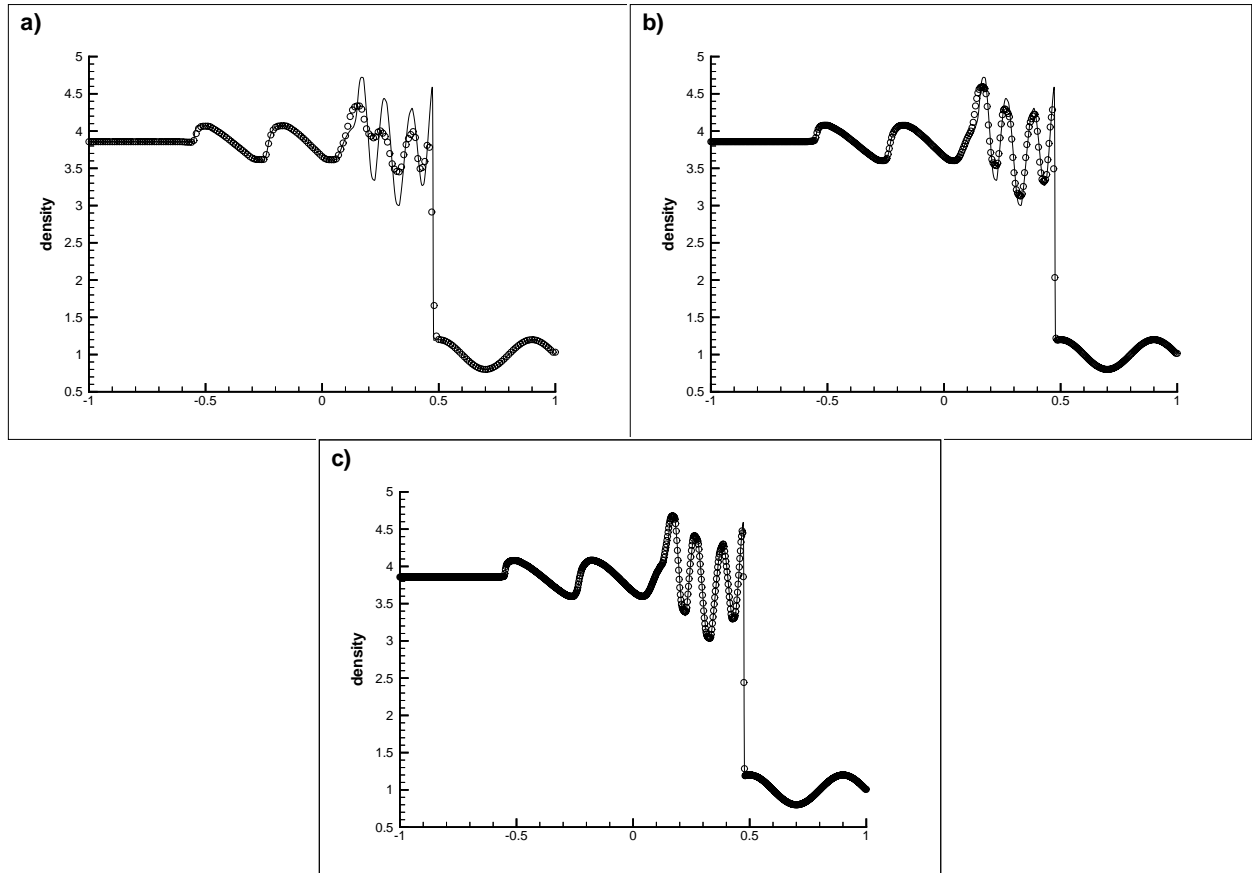


FIG. 10. Moving shock interacting with a sinusoidal disturbance in density: numerical solutions using grids of a) 200pts.; b) 400pts.; c) 800pts. Solid line on all the plots represents the numerical solution obtained 1600pts. grid.

- [11] P. L. ROE, *Approximate riemann solvers, parameter vectors, and difference schemes*, J. Comp. Phys., 43 (1981), pp. 357–372.
- [12] C.-W. SHU AND S. OSHER, *Efficient implementation of essentially non-oscillatory shock-capturing schemes*, J. Comp. Phys., 77 (1988), pp. 439–471.
- [13] D. SIDILKOVER, *Some approaches towards constructing optimally efficient multigrid solvers for the inviscid flow equations*. ICASE Report 97-39, Also to appear in *Computers & Fluids*.
- [14] —, *Numerical solution to steady-state problems with discontinuities*, PhD thesis, The Weizmann Institute of Science, Rehovot, Israel, 1989.
- [15] —, *A genuinely multidimensional upwind scheme and efficient multigrid solver for the compressible euler equations*, Report No. 94-84, ICASE, 1994.
- [16] —, *A genuinely multidimensional upwind scheme for the compressible euler equations*, in *Proceedings of the Fifth International Conference on Hyperbolic Problems: Theory, Numerics, Applications*, J. Glimm, M. J. Graham, J. W. Grove, and B. J. Plohr, eds., World Scientific, June 1994.
- [17] —, *Multidimensional upwinding and multigrid*. AIAA 95-1759, June 19-22, 1995. 12th AIAA CFD meeting, San Diego.
- [18] D. SIDILKOVER AND A. BRANDT, *Multigrid solution to steady-state 2d conservation laws*, SIAM J. Numer. Anal., 30 (1993), pp. 249–274.
- [19] D. SIDILKOVER AND P. L. ROE, *Unification of some advection schemes in two dimensions*, Report No.

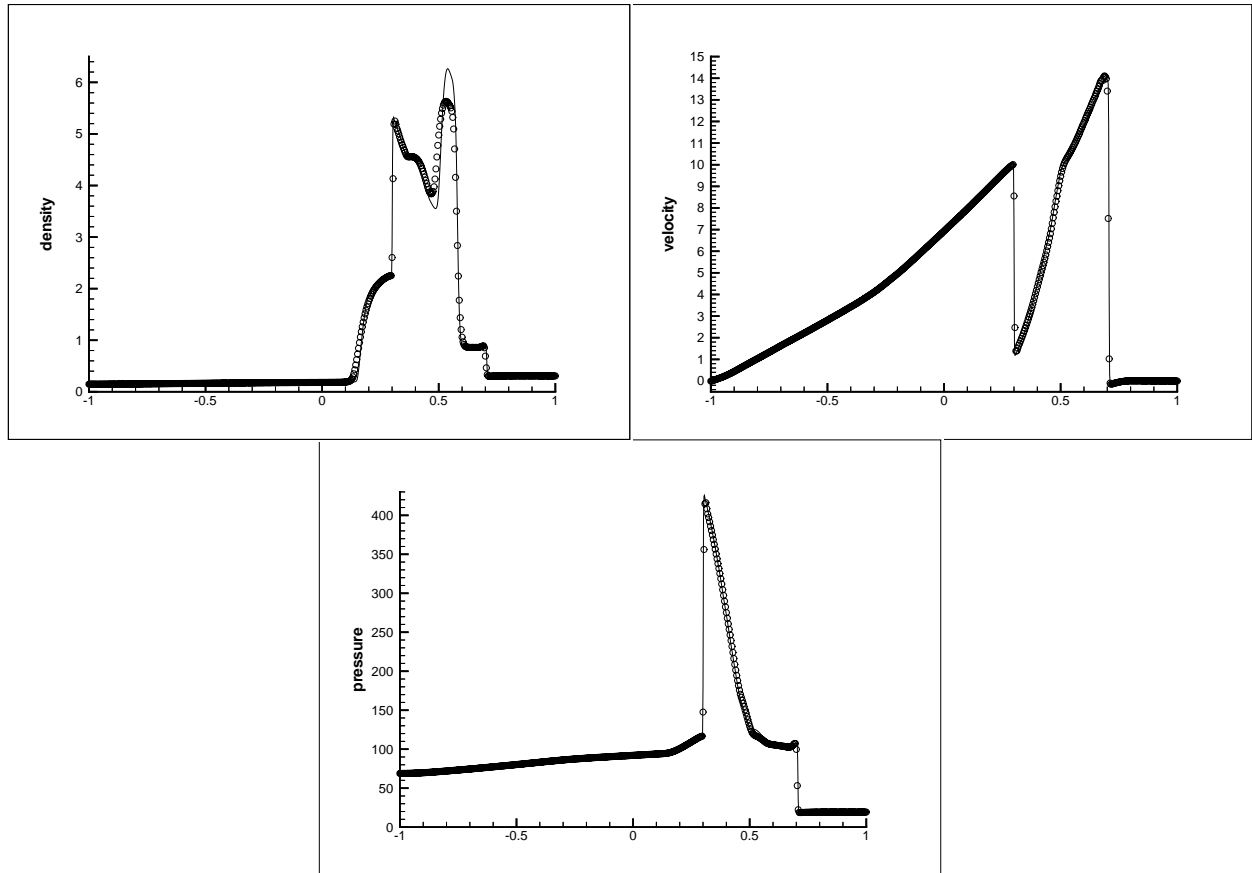


FIG. 11. *Colella-Woodward problem.* Numerical solution obtained on a grid of 500pts. is depicted by circles. The solid line corresponds to the numerical solution obtained on 1000pts. grid.

- 95-10, ICASE, 1995.
- [20] S. SPEKREIJSE, *Multigrid solution of monotone second-order discretization of hyperbolic conservation laws*, Math. Comp., 49 (1987), pp. 135–155.
  - [21] P. SWEBY, *High resolution schemes using flux limiters for hyperbolic conservation laws*, SIAM J. Numer. Anal., 21 (1984), pp. 995–1011.
  - [22] R. F. WARMING AND R. M. BEAM, *Upwind second order difference schemes and applications in aerodynamics*, AIAA Journal, 14 (1976), pp. 1241–1249.

## Appendix A. Residual-distribution (fluctuation-splitting) formulation.

The approach for constructing genuinely multidimensional upwind schemes for the Euler equations was formulated in [16],[15] in the residual-distribution context. Here we shall reformulate the scheme constructed in §2.3 in the same context as well.

The philosophy of this approach, proposed in [3] for scalar advection is that the discrete equation to be solved at each grid point is constructed from portions of the residuals (fluctuations) of the equation(s) evaluated on the grid elements (segments in one-dimensional case) adjacent to this grid point. The question of constructing a discrete scheme reduces to the question of defining a rule of distributing residuals to the nodes from a grid element.

**A.1. Scalar case.** Consider a scalar conservation law (2.1). Its residual on the segment  $[k, k + 1]$  (multiplied by the mesh-size) is given by

$$(A.1) \quad r = \Delta f_{k+\frac{1}{2}} = a_{k+\frac{1}{2}} \Delta u_{k+\frac{1}{2}}$$

The first order upwind scheme at the points  $k$  and  $k + 1$  can be given by the following residual distribution formulas

$$(A.2) \quad \begin{aligned} \Delta_t u_{k+1} &= \frac{1}{2} \lambda (r + \bar{r}) + C.O.L. \\ \Delta_t u_k &= \frac{1}{2} \lambda (r - \bar{r}) + C.O.L. \end{aligned}$$

where *C.O.L.* stands for *Contributions from Other Elements* and the term  $\bar{r}$  stands in this case for the artificial dissipation and is defined as follows

$$(A.3) \quad \bar{r} = \text{sign}(a_{k+\frac{1}{2}}) r = |a_{k+\frac{1}{2}}| \Delta u_{k+\frac{1}{2}}$$

The higher-resolution scheme identical to that presented in §2.3 can be obtained by defining

$$(A.4) \quad \bar{r} = \text{sign}(a_{k+\frac{1}{2}}) \left[ r + (1 - \nu_{k+\frac{1}{2}}) \left( \psi(q_k^+) a_{k+\frac{1}{2}}^+ + \psi(q_{k+1}^-) a_{k+\frac{1}{2}}^- \right) \Delta u_{k+\frac{1}{2}} \right]$$

where the quantities  $q_k^\pm, q_{k+1}^\pm, \nu_{k+\frac{1}{2}}$  are as defined in §2.3.

**A.2. Euler system.** The residual of the Euler system on the segment  $[k, k + 1]$  can be computed according to the following

$$(A.5) \quad \mathbf{r} = \Delta \mathbf{f}_{k+\frac{1}{2}} = \tilde{A}_{k+\frac{1}{2}} \Delta \mathbf{u}_{k+\frac{1}{2}}$$

By analogy to the scalar case, the first order upwind scheme is defined by the residual distribution formulas

$$(A.6) \quad \begin{aligned} \Delta \mathbf{u}_{k+1} &= \frac{1}{2} \lambda (\mathbf{r} + \bar{\mathbf{r}}) + C.O.L. \\ \Delta \mathbf{u}_k &= \frac{1}{2} \lambda (\mathbf{r} - \bar{\mathbf{r}}) + C.O.L. \end{aligned}$$

with

$$(A.7) \quad \bar{\mathbf{r}} = \text{sign}(\tilde{A}_{k+\frac{1}{2}}) \mathbf{r} = |\tilde{A}_{k+\frac{1}{2}}| \Delta \mathbf{u}_{k+\frac{1}{2}}.$$

The high-resolution scheme identical to one constructed in §4 can be obtained by the following definition

$$(A.8) \quad \bar{\mathbf{r}} = \text{sign}(\tilde{A}_{k+\frac{1}{2}}) \left[ \mathbf{r} + T^{-1} \mathbf{h}_{k+\frac{1}{2}}^{AD} \right].$$

Again, the notation used in (A.7) and (A.8) was established in §4.

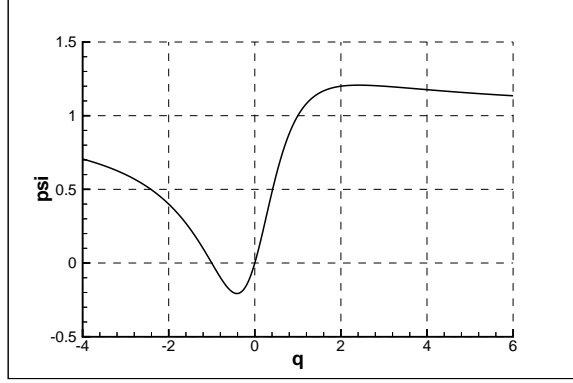


FIG. 12. *Van Albada limiter.*

**Appendix B. Van Albada limiter and TVD property.** Implicit solvers for steady-state or unsteady computations based on the high-resolution schemes are usually unable to drive residuals to the machine zero. The reason for this is the numerical fluxes that may be discontinuous due to the limiters. Limiters are based on the ratio of two quantities. A limiter function can be looked at as a function of two arguments: the numerator and denominator of this ratio. The limiter function that satisfies the “standard” TVD condition (see (2.29) or Fig.3) is a discontinuous function of its second argument (denominator of the ratio) at zero.

It is not clear whether or not the inability to obtain convergence of the residuals to the machine zero is a serious problem, since the “limit cycle” normally occurs when convergence below the level of truncation error is achieved. However, this difficulty can be easily removed by using a limiter function which satisfies the following requirement

$$(B.1) \quad \psi|_{+\infty} = \psi|_{-\infty}.$$

For instance, the Van Albada limiter, which is given by

$$(B.2) \quad \psi(q) = \frac{q^2 + q}{q^2 + 1}$$

(see also Fig.12), satisfies (B.1). The problem, however, seems to be that it does not satisfy the “standard” TVD condition (2.29).

Note that (2.29) is a *sufficient* condition for a high-resolution scheme to be TVD and, in fact, is too restrictive. A more general condition on the limiter in order to ensure the TVD property of the scheme is presented, for instance, in [20].

Here we shall just state that the following generalization of (2.29)

$$(B.3) \quad -\alpha \leq \psi(q) \leq 2 - \alpha, \quad -\alpha \leq \frac{\psi(q)}{q} \leq 2 - \alpha$$

with  $\alpha \geq 0$ , also implies the TVD property. The latter is quite clear from (2.42) in §2.2.2. A necessary condition for the second order accuracy is  $\alpha \leq 1$ .

It is obvious that the Van Albada limiter satisfies (B.3) with, for instance,  $\alpha = .5$ .